Flow Near the Meniscus of a Pressure-Driven Water Slug in Microchannels

Sungwook Kim

Samsung Advanced Institute of Technology,
Gyeongyi-do 449-901, Korea

Songwan Jin, Jung Yul Yoo*

School of Mechanical and Aerospace Engineering, Seoul National University,
Seoul 151-744, Korea

Micro-PIV system with a high speed CCD camera is used to measure the flow field near the advancing meniscus of a water slug in microchannels. Image shifting technique combined with meniscus detecting technique is proposed to measure the relative velocity of the liquid near the meniscus in a moving reference frame. The proposed method is applied to an advancing front of a slug in microchannels with rectangular cross section. In the case of hydrophilic channel, strong flow from the center to the side wall along the meniscus occurs, while in the case of the hydrophobic channel, the fluid flows in the opposite direction. Further, the velocity near the side wall is higher than the center region velocity, exhibiting the characteristics of a strong shear-driven flow. This phenomenon is explained to be due to the existence of small gaps between the slug and the channel wall at each capillary corner so that the gas flows through the gaps inducing high shear on the slug surface. Simulation of the shape of a static droplet inside a cubic cell obtained by using the Surface Evolver program is supportive of the existence of the gap at the rectangular capillary corners. The flow fields in the circular capillary, in which no such gap exists, are also measured. The results show that a similar flow pattern to that of the hydrophilic rectangular capillary (i.e., center-to-wall flow) is always exhibited regardless of the wettability of the channel wall, which is also indicative of the validity of the above-mentioned assertion.

Key Words : Microfluidics, Micro-PIV, Meniscus, Slug, Image Shifting Technique

1. Introduction

Over the past several years, as the understanding of microfluidics becomes more and more important in the design of microdevices, such as biochip, flow cytometer, capillary pumped loop (CPL), etc., a considerable number of theoretical and experimental studies have been performed

---
* Corresponding Author,
  E-mail : jyyoo@snu.ac.kr
  TEL : +82-2-880-7112; **FAX** : +82-2-883-0179
  Also at the Institute of Advanced Machinery and Design, Seoul National University, Seoul 151-744, Korea. (Manuscript **Received** August 25, 2005; **Revised** March 2, 2006)

on the capillary phenomena (Park et al., 2001 ; Höhmann and Stephan, 2002 ; Park et al., 2003 ; Buffone et al., 2004 ; Buffone and Sefiane, 2004a, 2004b).

Advance in the micro scale velocity measurement techniques, represented by micro-PIV, enables us to have a closer view of the micro scale flow. In particular, the flow near the meniscus is also one of the most important research topics regarding micro-scale heat transfer. Park et al. (2001) applied the MTFV (Molecular Tagging Fluorescence Velocimetry) to visualization of the three-dimensional flow occurring inside a heated capillary pore of 5-mm inner diameter with 5° inclination angle. The results show that the

thermocapillary stress plays an important role in the flow near the meniscus. Park et al.(2003) obtained optically-sectioned flow field mapping for the regions near an advancing bubble front, inside square microchannels using high-speed CLSM (Confocal Laser Scanning Microscopy) which suppresses all out-of-focus structures at image formation, thus eliminating the error caused by out-of-focus particle images in micro-PIV. The flow induced by naturally evaporating ethanol inside the glass capillary is also observed by Buffone et al.(2004).

However, the discrepancies between the known equations of capillary dynamics and the experimental results are still being reported. One reason of these discrepancies is thought to be the complexity of the actual flow near the meniscus in the capillary (Zhmud et al., 2000). Laminar flows in a pipe or a channel are usually characterized by a parabolic velocity profile, which for a capillary flow would hold far from the meniscus. However, it is obvious that the velocity profile is not parabolic near the meniscus. In particular, the flow pattern near the meniscus is expected to vary depending on the surface wettability, i.e., hydrophilicity or hydrophobicity because the shape of the meniscus also varies with it. The main objective of this study is to understand the fluid motion near the meniscus of a pressure-driven water slug advancing in microchannels with the rectangular and circular cross sections subject to hydrophilic and hydrophobic surface conditions, where micro-PIV technique is adopted to observe the flow structure and to obtain the velocity field near the meniscus. Because the pressure-driven water slug moves very fast, we apply time-resolved PIV setup (Sung and Yoo, 2001) which uses a high speed CCD camera. The problems arising from moving meniscus are overcome by fixing the meniscus position in the image using meniscus detection and image shifting technique.

2. Experimental Setup

A micro-PIV system, illustrated in Fig. 1, is assembled to measure instantaneous and time-averaged velocity field near the meniscus of a

pressure-driven water slug in microchannels. Unlike the usual micro-PIV system, a mercury lamp combined with green filter cube (Olympus U-MWG2) is used as the light source. The white light which comes from the mercury lamp is filtered so that only the green light passes through the bandpass filter. This green light is then reflected at the dichroic mirror mounted on the filter cube. The main problem with using a continuous light source, such as the mercury lamp, is that a particle is captured as a streak image not as a dot image. This problem depends on the flow velocity and camera exposure time. That is, the streak becomes longer as the velocity becomes higher and as the exposure time becomes longer. This can be successfully overcome by controlling the exposure time of the high speed CCD camera. Used high speed CCD camera (NAC Inc. PCI2000s) allows us to regulate the exposure time to be short enough so that it does not make any streak images. The maximum frame rate of this camera is 250 frames per second with maximum resolution of 480×420 pixels. Another important reason that we use a high speed CCD camera and continuous light source is because the meniscus moves very fast. Under our experimental condition, the meniscus escapes the field of view within a few seconds. Therefore, to get as much data as possible, it is more desirable to use a high speed camera and a continuous light source.
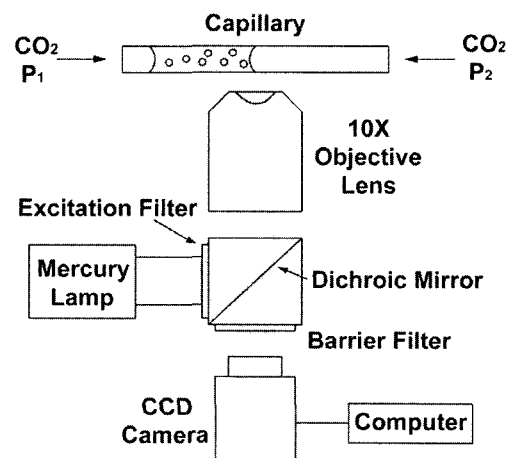
Fluorescent polystyrene microspheres of 1-μm

Fig. 1 A schematic of the experimental setup

or 0.5-μm in diameter, suspended in DI water, are used as seed particles. These fluorescent particles absorb green light ($\lambda_{a,max}$=542 nm) and emit red light ($\lambda_{e,max}$=612 nm). Olympus UPlanFl NA 0.3 10X objective lens mounted on an Olympus IX50 inverted epi-fluorescence microscope is used to take the fluorescent particle image. The emitted light by the fluorescent particle passes through the objective lens, the dichroic mirror and the barrier filter.

Glass capillaries with rectangular and circular cross sections (VitroCom Inc.) are used as the test microchannels. The cross section of the rectangular capillary is 400×40 μm and the diameter of the circular capillary is 410 μm.

Since the surface of the untreated glass is hydrophilic, the hydrophobic surface is obtained by exposing the glass capillary to a solution of OTS (octadecyltrichlorosilane) in hexadecane and then drying. It is known that the contact angle between the water and the OTS coated glass surface is approximately from 108° (Silnerzan et al., 1991) to 120° (Tretheway and Meinhart, 2002). The slug position and its moving velocity inside the capillary are controlled with the pressure difference between the two CO_2 chambers that are connected with both ends of the capillary, by adjusting metering valves installed on the respective chambers.

3. Result and Discussion

There are two different methods of measuring the relative velocity of fluid motion inside a slug with respect to the meniscus using PIV. The first is to subtract the meniscus velocity from the fluid velocity after measuring the two velocities separately. The second is to shift the correlation window by the same distance as the moving distance of the meniscus in the second frame image. The first method is more convenient and simple but it can not resolve the fluid motion very near the meniscus. In particular, the unresolved region is widened in the case when the meniscus moves very fast. Therefore, the second method is adopted in the present study. To shift the correlation window, the meniscus position should be defined

first. Figure 2 shows a sample image and the corresponding mean gray level. To detect the meniscus position, the gray level in the search band which is shown in Fig. 2(a) is averaged over the y-direction (lateral direction) to yield an image intensity profile as a function of x (longitudinal direction) (Fig. 2(b)). The position where the mean gray level exceeds a threshold value, which is 5 times larger than the background gray level, is defined as the meniscus position. After this detection process, images are shifted to make fixed meniscus images before the velocity calculation. In this step, bilinear interpolation method is applied to increase the spatial resolution. To minimize the effect of out-of-focus particles, dim particle images are eliminated according to a threshold gray level, which is 30% of the maximum intensity.
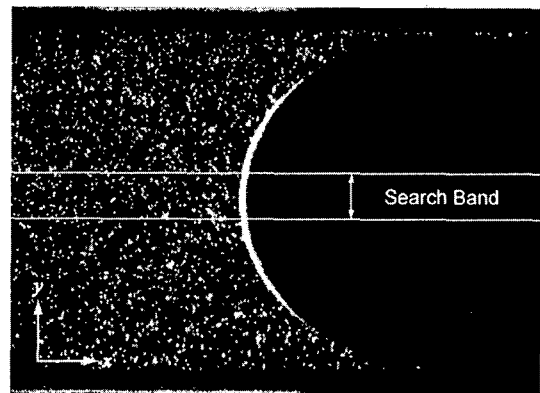
(a)
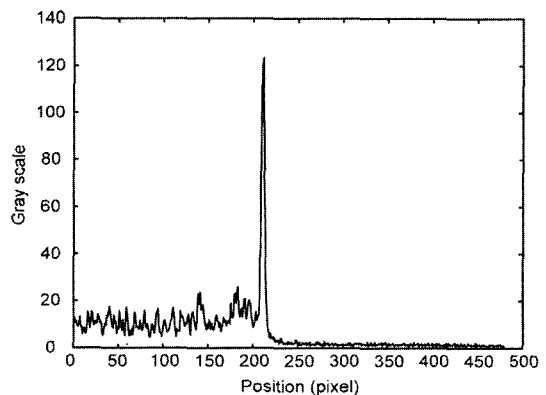
(b)

Fig. 2 Meniscus detection method : (a) Sample image, (b) Mean gray level as a function of x

The time-averaged velocity fields near the meniscus of an advancing slug in the rectangular microchannel are shown in Fig. 3, where about thirty instantaneous PIV velocity fields are ensemble-averaged in order to obtain velocity vectors relative to the meniscus are normalized by the meniscus velocity, u_m. We assume that the meniscus moves only by the pressure difference between both ends of the slug, not by the evaporation of water because the evaporation rate of confined water slug in a microchannel is known to be very small. In fact, the meniscus velocity which is derived from the evaporation is less than 1 μm/s when the slug does not move. Figures 3 (a) and 3 (b) are, respectively, the results ob-

tained for hydrophilic and hydrophobic channels. Only half of the flow field is shown because all flow motions are symmetric with respect to the channel center. The interrogation region is 16×16 pixels with 50% overlap, which yields a spatial resolution of 5.1×5.1 μm.

In the case of the hydrophilic channel, the fluid flows down towards the wall along the meniscus and back to the upstream (Fig. 3(a)). On the whole, it seems that the no-slip boundary condition is satisfied because the receding fluid velocity very near the wall is almost of the same magnitude as the meniscus velocity but of the opposite direction to it. In any event, this fluid motion near the meniscus is far from the fully-developed parabolic velocity profile. For the hydrophobic case, however, the fluid very near the wall flows in the opposite direction to that for the hydrophilic case. That is, a strong inward moving flow from the wall to the center along the meniscus is observed. Moreover, the near-wall velocity is higher than the channel center region velocity. There are many researches about slip boundary condition in the microchannel (Tretheway and Meinhart, 2002; Lauga and Stone, 2003; Jin et al., 2004), among which there is a fairly general agreement on the existence of the slip, particularly for the hydrophobic surface, although there are some variations of the amount of slip. But it is still very unusual that the near-wall velocity is higher than the center region velocity in the hydrophobic microchannel, even though we take account of the slip boundary condition. To better explain this anomaly, we conjecture that the wettability of the rectangular microchannel might work quite differently for the hydrophilic and hydrophobic walls.

Figure 4 is an illustration of the expected meniscus shape of a water slug, respectively, in a hydrophilic (Fig. 4(a)) and a hydrophobic (Fig. 4(b)) square microchannel. In the case of the hydrophilic channel, all four corners must be totally wetted with water. But it is likely that the corners are not wetted in the case of the hydrophobic channel. Under this condition, the pressurized CO_2 gas, which is used to control the slug position and velocity, flows through the gap bet-

$u_m = 386$ μm/s

200 μm
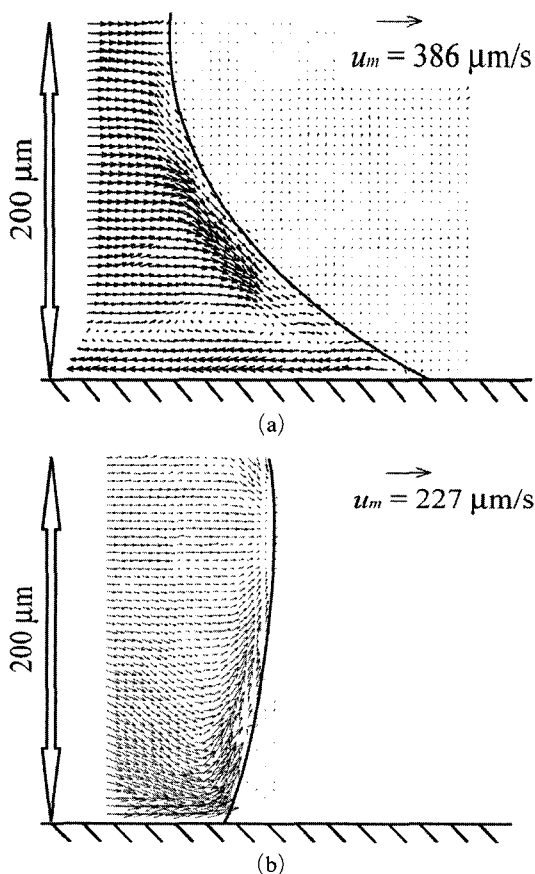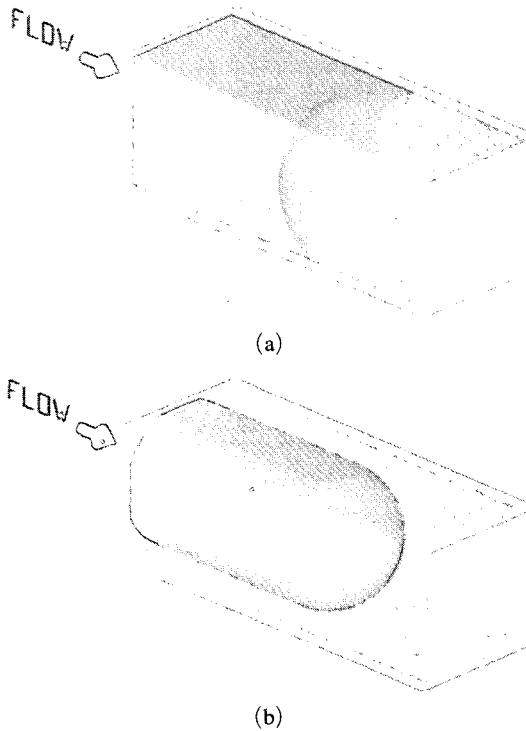
(a)

$u_m = 227$ μm/s

200 μm

(b)

Fig. 3 Time-averaged velocity fields near the meniscus of an advancing slug in a rectangular microchannel: (a) Hydrophilic surface, $u_m = 386$ μm/s, (b) Hydrophobic surface, $u_m = 227$ μm/s

(a)

(b)

Fig. 4 Illustration of the meniscus shapes in square microchannels: (a) Hydrophilic surface, (b) Hydrophobic surface

Fig. 5 Static droplet shape in a cubical cell of 1 mm $\times$ 1 mm $\times$ 1 mm with hydrophobic inner surface (simulation result using Surface Evolver program)

ween the slug and channel corners. This flow induces a high shear on the surface of the slug, generating additionally a shear-driven flow shown in Fig. 3(b) near the wall.

The water slug shape, which is situated statically in a cubical cell of 1 mm $\times$ 1 mm $\times$ 1 mm with hydrophobic inner surface, is numerically predicted by using Surface Evolver program (Brakke, 1992) which analyzes liquid surface shape with surface tension energy and other types of energy. We assume that the contact angle between the hydrophobic surface and the water is 120° and the gravitational force is negligible. As shown in Fig. 5, all corners are not fully wetted with water even though the gap between the liquid and the corner is very small. Although this simulation is for the case of a static droplet, we consider that the effect of surface tension is significant enough to maintain its shape even for the case of a moving droplet in the square or rectangular microchannels.

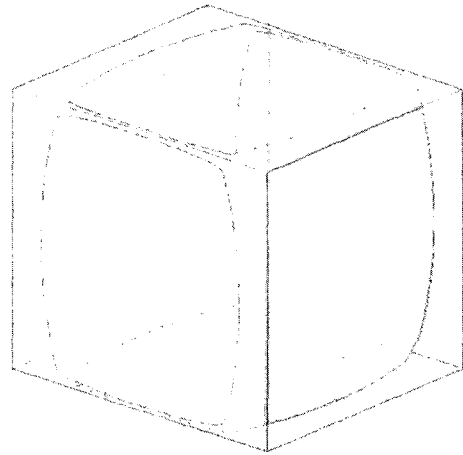On the other hand, it is obvious that such a

gap does not exist in the circular microchannels. There may be a small gap in the flow through a circular hydrophobic channel. Several studies report the existence of nanobubbles on the hydrophobic surface (Tyrrell and Attard, 2001). However, we think that the gap between the hydrophobic surface and the water is too small to transport the gas through the gap. The velocity fields inside the circular hydrophilic and hydrophobic channels of 410 μm in diameter are also measured in the same manner as those of the rectangular channels (Fig. 6(a) and 6(b)). Contrary to the results for the rectangular channels but in accordance with our assertion, both hydrophilic and hydrophobic channels exhibit similar flow patterns. That is, the fluid rotates in the same direction as in the hydrophilic rectangular channel regardless of the surface wettability. This result may not be a complete verification of our assertion that the corners are *not wetted in the hydrophobic rectangular channel*, but may serve as a guidance for better understanding of the flow phenomena in the rectangular or square microchannels.

The fact that the velocity fields shown in Fig. 3 do not satisfy the continuity condition implies that the flow is three-dimensional. Therefore, more detailed studies on the three-dimensional

flow structure near the meniscus and the effects of the surface characteristics are required. A micro-PIV utilizing CLSM would serve as a very powerful tool for investigating the three-dimensional flow structure in microchannels. Further study on the slug shape, particularly on the existence of the gap at the corner, is also important.

4. Conclusion

This study addresses the fluid motion near the meniscus of an advancing slug in microchannels with different surface characteristics. A micro-PIV system is used, which consists of an epi-fluorescence inverted microscope with a filter cube and a 10X oil-immersion objective, and a high speed CCD camera. To obtain the velocity field in a moving reference frame, the meniscus position is first detected by scanning the image pixels whose gray level exceeds a certain threshold value and then the particle images are shifted to constitute fixed-meniscus images. By this image-shifting technique, the fluid motions near the menisci of hydrophilic and hydrophobic microchannels can be apparently compared. The velocity field obtained in the moving reference frame shows that the near-wall velocity in the hydrophobic capillary is greater than that of the center region. We explain this phenomenon by asserting that there exist small but non-negligible gaps between the slug and the channel wall at the capillary corners. This assertion is supported by the measurement of the velocity field in the circular microchannel, and by the Surface Evolver simulation of a static droplet inside a cubical cell.

This result tells us an important information on the pressure loss in microchannels under different surface conditions. It is usually imagined that the water slug in the hydrophobic channel is easier to move because of the slip boundary condition. However, it might not be true if there are small gaps at the capillary corners and if we want to move the slug by using pressure difference. We cannot conclude that how much additional pressure is needed or whether a higher pressure is really needed to move the water slug in hydrophobic channels which have corners. In any event,

it is important to carefully consider the surface condition in designing a microfluidic system.

References

Brakke, K. A., 1992, "The Surface Evolver," *Experimental Mathematics*, Vol. 1, pp. 141~165.

Buffone, C., Sefiane, K. and Christy, J. R. E., 2004, "Experimental Investigation of the Hydrodynamics and Stability of an Evaporating Wetting Film Placed in a Temperature Gradient," *Applied Thermal Engineering*, Vol. 24, pp. 1157~1170.

Buffone, C., Sefiane, K., 2004a, "IR Measurements of Interfacial Temperature during Phase Change in a Confined Environment," *Experimental Thermal and Fluid Science*, Vol. 29, pp. 65~74.

Buffone, C., Sefiane, K., 2004b, "Investigation of Thermocapillary Convection Patterns and Their Role in the Enhancement of Evaporation from Pores," *International Journal of Multiphase Flow*, Vol. 30, pp. 1071~1091.

Höhmann, C., Stephan, P. C., 2002, "Microscale Temperature Measurement at an Evaporating Liquid Meniscus," *Experimental Thermal and Fluid Science*, Vol. 26, pp. 157~162.

Jin, S., Huang, P., Park, J., Yoo, J. Y. and Breuer, K. S., 2004, "Near-Surface Velocimetry Using Evanescent Wave Illumination," *Experiments in Fluids*, Vol. 37, pp. 825~833.

Lauga, E. and Stone, H. A., 2003, "Effective Slip in Pressure-Driven Stokes Flow," *Journal of Fluid Mechanics*, Vol. 489, pp. 55~77.

Park, J. S., Choi, C. K., Kihm, K. D. and Allen, J. S., 2003, "Optically-Sectioned Micro PIV Measurements Using CLSM," *Journal of Heat Transfer*, Vol. 125, p. 542.

Park, J. S., Kim, H. J. and Kihm, K. D., 2001, "Molecular Tagging Fluorescence Velocimetry

(MTFV) for Lagrangian Flow Field Mapping Inside Evaporating Meniscus : Potential Use for Micro-Scale Applications," *Journal of Flow Visualization and Image Processing*, Vol. 8, pp. 177~ 187.

Silnerzan, P., Leger, L., Ausserre, D. and Benattar, J. J., 1991, "Silanation of Silica Surfaces. A New Method of Constructing Pure or Mixed Monolayers," *Langmuir*, Vol. 7, pp. 1647~1651

Sung, J. and Yoo, J. Y., 2001, "Three-Dimensional Phase Averaging of Time-Resolved PIV Measurement Data," *Measurement Science and Technology*, Vol. 12, pp. 655~662.

Tretheway, D. C. and Meinhart, C. D., 2002, "Apparent Fluid Slip at Hydrophobic Microchannel Walls," *Physics of Fluids*, Vol. 14, No. 3, pp. L9~L12.

Tyrrell, J. W. G. and Attard, P., 2001, "Images of Nanobubbles on Hydrophobic Surfaces and Their Interactions," *Physical Review Letters*, Vol. 87, No. 17, 176104.

Zhmud, B. V., Tiberg, F. and Hallstensson, K., 2000, "Dynamics of Capillary Rise," *Journal of Colloid and Interface Science*, Vol. 228, pp. 263~ 269.